The modulus and elongation data are preliminary. Longer test specimens, which are not yet available, will be required to facilitate Instron testing at gauge lengths >2.5 cm and therefore to obtain representative modulus and elongation values.

In summary, strong, pure, and uniform carbon fibers were obtained by LCVD. The growth rates obtained with these fibers ($>300\ \mu m\ s^{-1}$) were comparable to those obtained with commercial melt-drawn sapphire fibers (*7*). Eventually, LCVD carbon fibers should therefore attain a price point comparable to that of melt-drawn sapphire fibers. As premium fibers, they may be suitable for currently emerging sensor markets, which have begun to use carbon fibers as functional electrical materials (*8*, *9*). For example, conventional carbon fibers were recently evaluated in Japan (*10*, *11*) and in the United States (*12*) as infrared detecting elements and intelligent infrared sensors, and the most desirable results were claimed for straight and coiled polyacrylonitrile-based carbon fibers (*12*). LCVD carbon fibers may have added value over incumbent carbon fibers because of their greater chemical purity and structural uniformity. In addition, the LCVD process can be modified to produce coiled fibers (*3*, *5*) if a coiled LCVD carbon fiber were required for a given end use.

REFERENCES

1. L. S. Nelson and N. L. Richardson, *Mater. Res. Bull.* 7, 971 (1972).
2. D. Bäuerle, *Chemical Processing with Lasers* (Springer-Verlag, Berlin, 1986), pp. 71, 93, and 224.
3. H. Westberg, M. Boman, A.-S. Norekrans, J.-O. Carlsson, *Thin Solid Films* **215**, 126 (1992).
4. G. G. Tibbetts, in *Carbon Fibers, Filaments and Composites*, J. L. Figueiredo, R. T. Baker, K. J. Hüttinger, Eds. (Kluwer, Dordrecht, Netherlands, 1990), pp. 73–94.
5. F. T. Wallenberger, lecture given at the International Workshop on Advances in Inorganic Fiber Technology, Melbourne, Australia, 13 and 14 August 1992; ______, P. C. Nordine, M. Boman, *Comp. Sci. Tech.*, in press.
6. F. T. Wallenberger and P. C. Nordine, *Mater. Lett.* **14**, 198 (1992).
7. J. T. A. Polluck, *J. Mater. Sci.* **7**, 787 (1972).
8. N. Muto *et al.*, *J. Mater. Sci. Lett.* **9**, 1269 (1990).
9. N. Muto *et al.*, *Sens. Mater.* **2**, 313 (1991).
10. H. Yanagida, in *Proc. Jpn. Ceram. Soc.* **81–90**, 81 (1991).
11. N. Muto *et al.*, *Denshi Joho Tsushin Gakkai Ronbunshi* **J74-CII**, 458 (1991).
12. C. D. E. Lakeman *et al.*, *Mater. Lett.* **13**, 330 (1992).

12 November 1992; accepted 13 January 1993

A Photoinduced Persistent Structural Transformation of the Special Pair of a Bacterial Reaction Center

N. Raja S. Reddy, Stephen V. Kolaczkowski, Gerald J. Small

Structural modification of photosynthetic reaction centers is an important approach for understanding their charge-separation processes. An unprecedented persistent structural transformation of the special pair (dimer) of bacteriochlorophyll molecules can be produced by light absorption alone. The nonphotochemical hole-burned spectra for the reaction center of *Rhodopseudomonas viridis* show that the phototransformation leads to a red shift of 150 wave numbers for the special pair's lowest energy absorption band, P960, and a comparable blue shift for a state at 850 nanometers, which can now be definitively assigned as being most closely associated with the upper dimer component. Additional insights on excited-state electronic structure include the identification of a new state.

The x-ray structures of the reaction center (RC) of the purple bacteria *Rhodopseudomonas viridis* (*1*) and *Rhodobacter sphaeroides* (*2*) have led to a burgeoning of experimental and theoretical activity directed toward an understanding of the primary charge-separation process (*3*, *4*). Although progress has been quite significant, important details are still controversial (*5*). That this is so, despite the availability of the RC structure, is a reflection of the complex and multifaceted nature of the problem; for example, a firm understanding of the electronically excited states of the RC is still lacking.

The two bacteriochlorophyll (BChl) monomers of the special pair (P) are closely juxtaposed; their pyrrole rings I overlap at an average macrocycle separation of $\sim$3.3 Å for *Rps. viridis*. Rings I of the two monomers are essentially perfectly overlapped with the Q_y transition dipoles making an angle of 139°. It is the lowest excited $\pi\pi^*(Q_y)$ state of P, denoted as P*, that is, the primary electron donor state. This state is also designated as P_- because the structure of the special pair mandates that it is the antisymmetric linear combination of the localized excitations, $P_MP_L^*$ and $P_M^*P_L$, within the excitonic dimer model (the subscripts M and L designate protein subunits). The upper dimer component is then P_+. The RC possesses a pseudo-C_2 symmetry axis that extends from P to the nonheme Fe. The other cofactors are, in order of proximity to P, $BChl_M$ and $BChl_L$; bacteriopheophytin$_M$ ($BPheo_M$) and $BPheo_L$; and finally, the two quinones, Q_M and Q_L.

We report nonphotochemical hole burning (NPHB) for the primary donor-state absorption profile of an RC, P960 of *Rps. viridis*. The resulting 4.2-K hole spectra for the entire Q_y absorption region (Fig. 1) are distinct from the transient photochemical hole-burned (PHB) spectra (*6–8*), for which the metastable population bottleneck state used is $P^+Q_L^-$. The NPHB spectra provide fresh insights into the nature of the states that absorb in the Q_y region and reveal a remarkable photoinduced structural transformation of the special pair.

Theoretical calculations based on the phenomenological exciton model (*9*, *10*) and semiempirical quantum chemical methods (*11–13*), in which varying degrees of parameterization are used, have demonstrated that interactions between the six chromophores (quinones can be excluded) of the RC are required for an adequate description of the Q_y states. Although there is general agreement that the lowest energy excited state (P960* in *Rps. viridis*) (Fig. 2) is predominantly the lower energy excitonic component of P (P_- as defined above), the assignment of P_+ in the absorption spectrum is more problematic. Such an assignment may not even be sensible because the Q_y states higher in energy than P_- can be expected to be chromophorically mixed (*9–13*). The phenomenological exciton model does not include charge-transfer states, such as $P^+\ BChl_{M/L}^-$, and charge-resonance states ($P_M^+P_L^-$ and $P_M^-P_L^+$), which are important not only to the dynamics of charge separation (*3*, *14*) but also to the energies and physical properties, such as the permanent dipole moment (*15*) of the states absorbing in the Q_y region of the absorption spectrum.

The principles of persistent NPHB of electronic transitions in amorphous solids such as glasses and polymers have been extensively reviewed (*16*). The NPHB technique has recently been applied to the Q_y transitions of Chls of a wide variety of antenna protein complexes (*17–21*). Briefly, NPHB takes advantage of the inherent structural disorder of amorphous solids [proteins are glasslike (*22*)]. This disorder leads to significant inhomogeneous broadening ($\Gamma_I \sim 100$ to $200\ cm^{-1}$) of the optical absorption transition. In NPHB (*23*), selective excitation of an "isochromat" with a narrow line laser ($<<\Gamma_I$), followed by re-

---

Ames Laboratory and Department of Chemistry, Iowa State University, Ames, IA 50011.

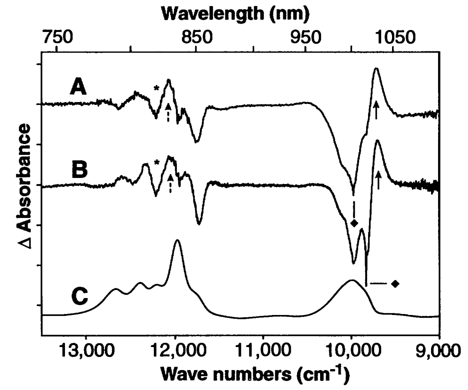

Fig. 1. Nonphotochemical hole-burned (NPHB) spectra. Burn laser frequencies were 9971 cm^{-1} (spectrum A) and 9831 cm^{-1} (spectrum B). Solid diamonds locate the zero-phonon hole (ZPH) at the burn frequency. Solid arrows identify the red-shifted anti-hole caused by a burn in the P960 state. Dashed arrows refer to the anti-hole generated by a burn of the 850-nm band. Asterisks locate the hole in the 818-nm band. The absorption spectrum (C) is included as a guide. Note the positive correlation of the position of the hole minimum of the 850-nm state with the burn frequency and the shift of the center of gravity of the P960 hole. Burn fluences were 250 mW cm^{-2} for 15 min (spectrum A) and 250 mW cm^{-2} for 30 min (spectrum B). The burn fluences are about a factor of 15 higher than those used in our earlier studies (*7*). Pre- and post-burn absorption spectra were obtained with a Bruker Instruments (Billerica, Massachusetts) 120HR Fourier-transform infrared (visible) spectrometer at a read resolution of 4 cm^{-1}. The sample was cooled to 4.2 K in a Janis Model 8-DT liquid-helium cryostat. A Coherent Inc. (Palo Alto, California) Ti:Sapphire laser pumped by a Coherent Inc. Innova 200 Ar$^+$ laser was used. See (*19*) for further experimental details and (*7*) for sample preparation. Optical density of the P960 band was 0.35.

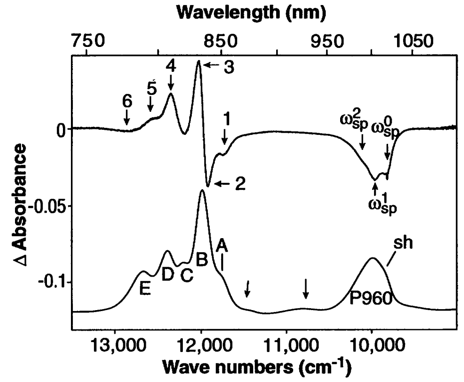

Fig. 2. Transient photochemical hole-burned (PHB) spectrum (top) and absorption spectrum (bottom) in the Q_y region of the *Rps. viridis* RC. The P960 is the lowest excitonic state of the special pair P, and "sh" refers to the origin band (ω^0_{sp}) of the marker mode Franck-Condon progression, ω^1_{sp} and ω^2_{sp}, identified in the top plot. Features A to E correspond to the other Q_y states of the RC. Burn conditions for PHB spectrum: ω_B = 9810 cm^{-1}, burn intensity = 100 mW cm^{-2}. The sharp but weak ZPH at the burn laser frequency is located by the ω^0_{sp} arrow. Feature 1 is a hole in the 850-nm band. Features 2 and 3 result from the shift of the B absorption band and features 4 to 6 result from the shift of the D and E bands.

laxation of the excited isochromat back to the electronic ground state, produces persistent chromophore-glass cage configurations that differ from their pre-excitation (preburn) configurations. This difference shifts the transition frequencies of the originally excited sites to other regions of the inhomogeneously broadened absorption profile, producing what is referred to as the anti-hole. The site-excitation selective bleaching of the zero-phonon lines coincident with the laser burn frequency, ω_B, produces the zero-phonon hole (ZPH), which is generally accompanied by relatively broad companion phonon side-band holes (PSBHs) to higher and lower energy of the ZPH at $\omega_B \pm \omega_m$, with $\omega_m \approx 20$ to 30 cm^{-1} (*17, 21*). The PSBHs are a manifestation of linear electron-phonon coupling whose strength is defined by the Huang-Rhys factor S (for weak coupling and strong coupling, $S < 1$ and $S > 1$, respectively). The theory of hole profiles (*24*) has been successfully applied to the photochemical hole profiles of P960 and P870 of *Rb. sphaeroides* (*7*) as well as the primary donor profile, P700, of the RC of photosystem I (*25*) and P680 of the photosystem II RC (*26*).

What is the nature of the NPHB spectrum when the excited electronic states are collective states of an aggregate of coupled chromophores, that is, the situation posed by the six cofactors of the RC? Recently, this question has been explored for the base-plate BChl *a* antenna protein complex of *Prosthecochloris aestuarii* (*18*) and the B800-B850 and B875 antenna complexes of *Rb. sphaeroides* (*19, 20*). The basic structural subunits of the base-plate complex (*27*), B850 and B875 (*28*), contain several excitonically coupled BChl *a* molecules (*27*). In the case of *P. aestuarii*, the resulting delocalized unit cell states give rise to several partially resolved Q_y bands in the 4.2 K absorption spectrum. Burning a hole at 4.2 K into the lowest energy band produces persistent satellite holes in the higher energy absorption bands (*18*). This response is expected when the states are linear combinations of the localized excited states of the individual chromophores because the change in the excitation energy of one (or more) of the chromophores, produced by an alteration of structure, changes the energies of the delocalized states (*18*). This point is important for what follows.

The features of interest in the absorption spectrum (Fig. 2) of the *Rps. viridis* RC samples that we used are P960 and bands A to E. The 4.2 K spectrum shown is essentially the same as our previously published spectra (*7*). Band C is not resolved in low-temperature spectra of poorer quality (broader bandwidths) and has been generally ignored or attributed to an impurity (*29*). The NPHB results presented below show that it is actually an intrinsic feature of the RC.

Photochemical hole burning studies of P960 show that the low-energy shoulder of P960 in Fig. 2 is the origin band (ω^0_{sp}) of a Franck-Condon progression of a mode unique to the special pair with ω_{sp} = 135 cm^{-1} and S_{sp} = 1.1 (*21*). We have referred to it as the special pair "marker" mode. The maximum of P960 is close to the one-quantum transition of ω_{sp} (ω^1_{sp}). The P960 transition also couples strongly to low-frequency phonons with a mean frequency of ~25 cm^{-1} and an S = 2.1. Thus, P960 is much broader than the higher energy Q_y bands because it couples strongly to these other modes.

Linear dichroism and circular dichroism studies (*29, 30*) and transient absorption measurements (*31*), as well as the observation of a positive correlation of site-excitation energies by hole burning (*6–8*), have implicated band A as a likely candidate for P_+ (the upper dimer component). Band B has been assumed by experimentalists to be attributable to degenerate localized transitions of BChl$_L$ and BChl$_M$, although theoretical calculations predict a number of different transitions in which significant mixing occurs between the Q_y transitions of the six cofactors (*9–13*). Band C lies in a region of the spectrum of considerable importance to the interpretation of ultrafast transient absorption data (*31*). The assignments of bands D and E as more or less pure BPheo$_L$ and BPheo$_M$ Q_y transitions are supported by all calculations except those of Thompson and Zerner (*13*). Their work, however, is a notable exception because it uses no parameterization beyond that required to describe the electronic states of monomers. Thompson and Zerner emphasized that the description of the states in the 750- to 850-nm region is difficult because of the close proximity of the zero-order states. They concluded, however, that the shoulder state at ~850 nm (Fig. 2, band A) is primarily P_+ (mainly excitonic but with some charge-resonance character).

In our PHB spectrum (Fig. 2), one observes for the P960 hole profile the weak (highly Franck-Condon forbidden) ZPH coincident with ω_B plus the marker mode progression (ω^0_{sp}, ω^1_{sp}, and ω^2_{sp}). Features 2 and 3 result from the shifting of the B absorption band. Features 4 to 6 result from shifting of the D and E absorption bands.

The shifting of the bands is caused by the formation of the $P^+ Q^-$ state (*32*). Feature 1 appears to be more of a bleach (hole) of the 850-nm (A) band than a manifestation of band shifting (*6, 29*). That feature 1 is a hole is firmly established by the NPHB spectra (Fig. 1). These hole spectra (corresponding to a 2% change in optical density for P960), together with spectra obtained as a function of burn fluence with several different ω_B values (not shown), establish that the 850-nm nonphotochemical hole is second only to the P960 hole in intensity.

The P960 anti-hole of the NPHB spectra (Fig. 1, solid arrow) is substantially red-shifted (150 cm^{-1}) relative to the low-energy shoulder (ω^0_{sp}) of the P960 absorption and PHB profiles. An important question is whether the anti-hole profile observed is actually ω^0_{sp} with ω^1_{sp} and ω^2_{sp} masked by interference with the P960 hole profile. The significant difference that we observe between the photochemical and nonphotochemical P960 profiles suggests that this is the case. We confirmed this result by normalizing the two profiles (for the same ω_B) to the same intensities over a frequency interval appropriately located on the high-energy tail of the hole profiles and subtracting. The resulting, somewhat line-narrowed difference spectrum exhibits the special-pair marker mode progression for the phototransformed P960 with $\omega_{sp} \simeq 140$ cm^{-1} and $S_{sp} \approx 1$ (Fig. 3). These values are, within experimental uncertainty, identical to those obtained from PHB spectra for P960 (*7, 20*). Therefore, the structural transformation of the special pair (see below) that is produced as the result of NPHB does not significantly alter the coupling of P_- (P960*) to the marker mode.

In the higher energy region of the NPHB spectra, the anti-hole of the 850-nm hole can be identified by inspection (Fig. 1, dashed arrow). The anti-hole is interfered with on its low-energy side by a relatively weak hole from band B (Fig. 2), which makes precise determination of the anti-hole maximum difficult. However, our NPHB studies of B850 and B875 of the *Rb. sphaeroides* antenna (*19, 20*) have shown that twice the energy difference between the maximum of the hole and the zero-crossing point of the hole spectrum is an accurate measure of the splitting between the hole and anti-hole. This procedure yields a value of $\sim +150$ cm^{-1} for the anti-hole maximum relative to the minimum of the 850-nm hole. This shift is equal in magnitude but opposite in sign to that observed for P960 (P_-). This is consistent with the simple excitonic dimer model when the structural change of the dimer alters primarily the excitonic coupling, that is, when change in the dispersion (*D*) term of exciton theory (*33*) is negligible.

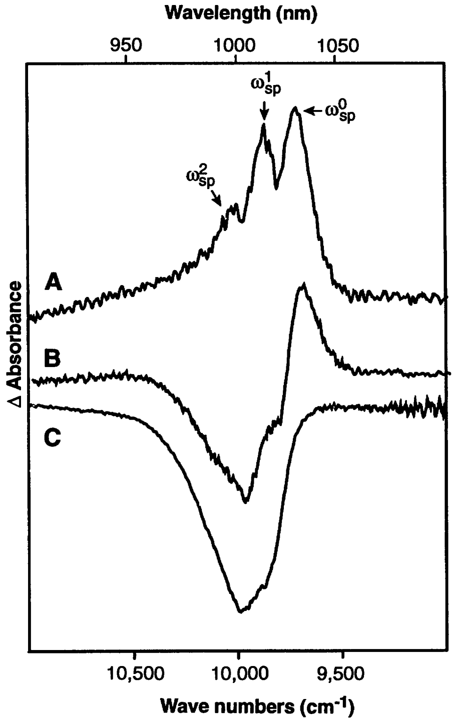

Fig. 3. Absorption of the phototransformed P960 is characterized by the marker mode progression and is evident in the difference spectrum (A), which comes from the NPHB spectrum (B) minus the transient PHB spectrum (C). Burn frequency was 10,790 cm^{-1}.

Our linearly polarized PHB spectra (not shown) are in essential agreement with the linear-dichroism data of Breton (*30*), but caution must be exercised in the assignment of the 850-nm state as P_+ solely on the basis of linear dichroism data. For example, the semiempirical calculations of Parson and Warshel (*11*) or excitonic calculations of Knapp *et al.* (*9*) do not lead to an unambiguous assignment of the 850-nm state to P_+, and yet the calculations account reasonably well for the linear and circular dichroism results. Therefore, for further guidance, we looked to the ratios (*R*) of the amplitudes of the nonphotochemical holes in the region of 750 to 850 nm (produced when we burn into P960) relative to the intensity of their respective absorption bands. Elsewhere we argue (*34*), on theoretical grounds, that these ratios, when compared to the corresponding ratio for P960, should provide a reasonable estimate of the contribution from P_L* and P_M* to the states in the above region. The analysis does require, in part, an accurate deconvolution of the contributions from bands A to E to the absorption spectrum, which can be accomplished with the aid of the NPHB and PHB spectra. The *R* values for bands A to E are 0.9, 0.03, 0.36, 0.05, and 0.09, respectively; the value of *R* for P960 is defined as 1.0.

Our theoretical analysis of the absorption and NPHB spectra (*34*) leads to the following findings: (i) in the 850-nm state there is a heavy contribution from P_L* and P_M* with occupation numbers similar to those of P_-; (ii) the 818-nm state (band C) also carries a significant contribution from $P_{L/M}$* but less so by a factor of 2 (Fig. 1, asterisks); and (iii) the states corresponding to bands B, D, and E have a much smaller contribution from $P_{L/M}$*. The above results establish that the 818-nm state is an intrinsic state of the RC. Together with the observation that the anti-hole of the 850-nm state is blue-shifted by the same amount (~ 150 cm^{-1}) that the anti-hole of P960 is red-shifted (negative correlation), the results provide convincing evidence that the 850-nm state corresponds very closely to P_+, the dimer partner of P_-.

We can also conclude that the structural transformation associated with the NPHB of P960 is highly localized on the special pair because our earlier PHB studies (*6, 8*) showed that the distributions of the site excitation energy for P960 and the 850-nm state are positively correlated (see legend to Fig. 1). This positive correlation suggests that the inhomogeneous broadenings of the P960 and 850-nm bands stem primarily from statistical fluctuations in inner- and outer-shell protein structure around the special pair rather than a distribution of structures for the special pair itself. Our NPHB spectra also show that the special pair marker mode (ω_{sp}), which couples strongly to P_-, is at most only weakly coupled to the 850-nm state. This is also apparent from the low-temperature difference spectrum obtained from the absorption of the normal (dark-adapted) and oxidized (P_+) RC by Vermeglio and Paillotin (*29*). The absence of coupling for the 850-nm state is significant because the simple excitonic dimer model predicts, for a dimer splitting $>> \omega_{sp}$, that the marker mode is equally active for both P_+ and P_- (*33*). That this is not the case strongly indicates that P_- is made unique from P_+ by virtue of more mixing of its zero-order exciton state with charge-transfer and charge-resonance states. Such mixing is suggested also by the results of Stark measurements, which show that the change in permanent dipole moment for the $P_- \leftarrow P$ absorption transition is large relative to those of the other transitions in the Q_y region (*12*). Strong linear electron-phonon coupling of P960 is accompanied by a large change in dipole moment (*21*).

The spectra presented lead to an adiabatic splitting between the zero-point levels of P_- and the 850-nm state (P_+) of ~ 1930 cm^{-1} at 4.2 K that is increased to ~ 2230 cm^{-1} for the phototransformed special pair. This increase of ~ 300 cm^{-1} for the "dimer" splitting could be caused by a $\sim$0.5 Å decrease in the 7.0 Å separation of Mg atoms in the special pair (*1*) (prediction of the simple exciton model with the dipole-dipole approximation). The calculations of Thompson and Fajer (*36*), which take into account the charge-resonance states of P, indicate that the observed blue and red shifts (150 cm^{-1}) of P_+ and P_- are not simply a result of the reduction of the average macrocycle separation distance. Higher level calculations, which take into account, for example, the ruffling of the macrocycles and the orientation of the ring I acetyl group (*37*), may provide plausible structures for the "new special pair."

REFERENCES AND NOTES

1. J. Deisenhofer, O. Epp, K. Miki, R. Huber, H. Michel, *J. Mol. Biol.* **180**, 385 (1984); *Nature* **318**, 618 (1985).
2. C. H. Chang *et al.*, *FEBS Lett.* **205**, 82 (1986).
3. R. A. Friesner and Y. Won, *Biochim. Biophys. Acta* **977**, 99 (1989).
4. C. Kirmaier and D. Holten, *Photosynth. Res.* **13**, 225 (1987); J. R. Norris and M. Schiffer, *Chem. Eng. News* **68**, 22 (30 July 1990).
5. D. Holten and C. Kirmaier, *Proc. Natl. Acad. Sci. U.S.A.* **87**, 3552 (1990); C. Lauterwasser, U. Finkele, H. Scheer, W. Zinth, *Chem. Phys. Lett.* **183**, 471 (1991); M. H. Vos *et al.*, *Proc. Natl. Acad. Sci. U.S.A.* **88**, 8885 (1991).
6. D. Tang, R. Jankowiak, J. M. Hayes, G. J. Small, D. M. Tiede in *Perspectives in Photosynthesis: Proceedings of the Twenty-Second Jerusalem Symposium on Quantum Chemistry and Biochemistry*, J. Jortner and B. Pullman, Eds. (Kluwer Academic, Dordrecht, Netherlands, 1990), pp. 99–120.
7. S. G. Johnson *et al.*, *J. Phys. Chem.* **94**, 5849 (1990) and references therein.
8. S. G. Johnson *et al.*, *ibid.* **93**, 5953 (1989).
9. E. W. Knapp, P. O. J. Scherer, S. F. Fischer, *Biochim. Biophys. Acta* **852**, 295 (1986).
10. Y. Won and R. A. Friesner, *J. Phys. Chem.* **92**, 2214 (1988).
11. W. W. Parson and A. Warshel, *J. Am. Chem. Soc.* **109**, 6152 (1987).
12. P. O. J. Scherer and S. F. Fischer, *Chem. Phys.* **131**, 115 (1989).
13. M. A. Thompson and M. C. Zerner, *J. Am. Chem. Soc.* **113**, 8210 (1991).
14. E. C. Kellogg, S. Kolaczkowski, M. Wasielewski, D. M. Tiede, *Photosynth. Res.* **22**, 47 (1989); D. E. Budil, P. Gast, C. H. Chang, M. Schiffer, J. Norris, *Annu. Rev. Phys. Chem.* **38**, 561 (1987).
15. D. J. Lockhart, S. L. Hammes, S. Franzen, S. G. Boxer, *J. Phys. Chem.* **95**, 2217 (1991).
16. J. M. Hayes, R. Jankowiak, G. J. Small, in *Persistent Spectral Hole-Burning: Science and Application*, vol. 44 of *Topics in Current Physics*, W. E. Moerner, Ed. (Springer-Verlag, New York, 1988), pp. 153–202; R. Jankowiak and G. J. Small, *Science* **237**, 618 (1987).
17. J. K. Gillie, G. J. Small, J. H. Golbeck, *J. Phys. Chem.* **93**, 1620 (1989).
18. S. G. Johnson and G. J. Small, *ibid.* **95**, 471 (1991).
19. N. R. S. Reddy, G. J. Small, M. Seibert, R. Picorel, *Chem. Phys. Lett.* **181**, 391 (1991).
20. N. R. S. Reddy and G. J. Small, *J. Chem. Phys.* **94**, 7545 (1991).
21. N. R. S. Reddy, P. A. Lyle, G. J. Small, *Photosynth. Res.* **31**, 167 (1992) and references therein.
22. I.-S. Yang and A. C. Anderson, *Phys. Rev. B* **34**, 2942 (1986); H. Frauenfelder, S. G. Sligar, P. G. Wolynes, *Science* **254**, 1598 (1991).
23. J. M. Hayes and G. J. Small, *Chem. Phys.* **27**, 151 (1978); L. Shu and G. J. Small, *ibid.* **41**, 447 (1990).
24. I.-J. Lee, J. M. Hayes, G. J. Small, *J. Chem. Phys.* **91**, 3463 (1989); J. M. Hayes, J. K. Gillie, D. Tang, G. J. Small, *Biochim. Biophys. Acta* **932**, 287 (1988).
25. J. K. Gillie, P. A. Lyle, G. J. Small, J. H. Golbeck, *Photosynth. Res.* **22**, 233 (1989).
26. R. Jankowiak, D. Tang, G. J. Small, M. Seibert, *J. Phys. Chem.* **93**, 1649 (1989).
27. R. M. Pearlstein, in *Chlorophylls*, H. Scheer, Ed. (CRC Press, Boca Raton, FL, 1991), pp. 1047–1078.
28. H. Zuber and R. A. Brunisholz, *ibid.*, pp. 627–703.
29. A. Vermeglio and G. Paillotin, *Biochim. Biophys. Acta* **681**, 32 (1982).
30. J. Breton, *ibid.* **810**, 235 (1985).
31. ———, J.-L. Martin, G. R. Fleming, J. C. Lambry, *Biochemistry* **27**, 8276 (1988).
32. L. K. Hanson, J. Fajer, M. A. Thompson, M. C. Zerner, *J. Am. Chem. Soc.* **109**, 4728 (1987).
33. R. M. Hochstrasser, *Molecular Aspects of Symmetry* (Benjamin, New York, 1966), pp. 307–331.
34. N. R. S. Reddy, S. V. Kolaczkowski, G. J. Small, in preparation.
35. M. A. Thompson, M. C. Zerner, J. Fajer, *J. Phys. Chem.* **95**, 5693 (1991).
36. M. A. Thompson and J. Fajer, *ibid.* **96**, 2933 (1992).
37. E. Gudowska-Nowak, M. D. Newton, J. Fajer, *ibid.* **94**, 5795 (1990).
38. Research at the Ames Laboratory was supported by the Division of Chemical Science, Office of Basic Energy Science, U.S. Department of Energy. Ames Laboratory is operated for the U.S. Department of Energy by Iowa State University under contract W-7405-Eng-82. We thank D. M. Tiede of the Argonne National Laboratory for providing the samples of the *Rps. viridis* RC.

5 November 1992; accepted 21 January 1993

Evidence for Photochemical Formation of H_2O_2 and Oxidation of SO_2 in Authentic Fog Water

Yuegang Zuo* and Jürg Hoigné

When samples of rain and fog water were exposed to ultraviolet and visible light, reactive transients such as hydrogen peroxide were formed and dissolved organic matter and sulfur dioxide were depleted. These results, in conjunction with those from previous studies, imply that dissolved organic compounds and transition metals such as iron ions are involved in the photochemical formation of hydrogen peroxide and other photooxidants in atmospheric waters.

Hydrogen peroxide (H_2O_2) is a key component in the conversion of dissolved sulfur dioxide (SO_2) to sulfuric acid (H_2SO_4), which is a main contributor to acid precipitation (*1–5*). Therefore, there is a great deal of interest in understanding the mechanisms responsible for the formation and degradation of H_2O_2 in the atmospheric liquids. We present evidence for the efficient iron-catalyzed photochemical generation of H_2O_2, the oxidation of dissolved SO_2, and the depletion of oxalic acid and other organic pollutants in fog water.

The occurrence of H_2O_2 in atmospheric water droplets is currently thought to be attributable to the dissolution of gaseous H_2O_2 and disproportionation of HO_2 radicals, which are also scavenged from the gas phase (*6–9*). Recently, however, it has been reported that H_2O_2 is formed by the photolysis of complexes of Fe(III) with oxalic, glyoxalic, and pyruvic acids under the conditions typical of acidified atmospheric waters (*10–13*). The mechanism of the photochemical formation of H_2O_2 is

$$\text{Fe(III)-L} \xrightarrow{h\nu} \text{Fe(II)} + \text{L}^{\cdot} \qquad (1)$$

$$\text{L}^{\cdot} + O_2 \rightarrow O_2^{\cdot\,-} + \text{oxidized L} \qquad (2)$$

$$2O_2^{\cdot -} + 2H^+ \rightarrow H_2O_2 + O_2 \qquad (3)$$

where $h\nu$ is the energy of a photon, L stands for organic ligands, and $\text{L}^{\cdot}$ for an organic radical.

The absorption of a photon by an Fe(III)-organo complex [Fe(III)-L] results in electron transfer from an organic ligand to the ferric ion, producing a ferrous ion and an organic radical. In the presence of O_2, the organic radical can reduce O_2 to form a superoxide ion ($O_2^{\cdot -}$). The $O_2^{\cdot -}$ and its conjugate acid, the hydroperoxyl radical ($HO_2^{\cdot}$), readily undergo a disproportionation reaction to yield H_2O_2 and O_2 in aqueous solutions (*14*).

Dissolved iron species and organic ligands, such as oxalic, pyruvic, and glyoxalic acids, are common constituents of cloud, rain, and fog droplets (*12, 15–22*). Speciation calculations (*10–13*) have shown that the Fe(III) exists predominantly in complexed forms with organic ligands. Therefore, it is reasonable to postulate that $HO_2^{\cdot}/O_2^{\cdot -}$ and its reaction product, H_2O_2, may also be photochemically formed in atmospheric waters by the above mechanism.

To test this postulation, we collected rain, snow, and fog waters in Dübendorf, Switzerland, and stored them at 4°C until used. The samples were filtered (0.45 μm) and analyzed immediately before irradiation. We observed the photochemical gen-

---

Swiss Federal Institute for Water Resources and Water Pollution Control (EAWAG), Swiss Federal Institute of Technology, ETHZ, CH-8600 Dübendorf, Switzerland.

*To whom correspondence should be addressed, at Drinking Water Research Center, Florida International University, Miami, FL 33199.